Talanta 122 (2014) 145–150

Contents lists available at ScienceDirect

Talanta

journal homepage: www.elsevier.com/locate/talanta

A novel method for evaluating flavanols in grape seeds by near infrared hyperspectral imaging

Francisco J. Rodríguez-Pulido, José Miguel Hernández-Hierro, Julio Nogales-Bueno, Belén Gordillo, M. Lourdes González-Miret, Francisco J. Heredia *

Food Colour & Quality Lab., Dept. Nutrition & Food Science, Facultad de Farmacia, Universidad de Sevilla, 41012-Sevilla, Spain

ARTICLE INFO

Article history:
Received 26 July 2013
Received in revised form
15 January 2014
Accepted 20 January 2014
Available online 30 January 2014

Keywords:
Chemometrics
Flavanols
Grape seeds
Hyperspectral imaging
Near infrared
Vitis vinifera L

ABSTRACT

Chemical composition of seeds changes during grape ripening and this affects the sensory properties of wine. In order to control the features of wines, the condition of seeds is becoming an important factor for deciding the moment of harvesting by winemakers. Sensory analysis is not easy to carry out and chemical analysis needs lengthy procedures, reagents, and it is destructive and time-consuming. In the present work, near infrared hyperspectral imaging has been used to determine flavanols in seeds of red (cv. Tempranillo) and white (cv. Zalema) grapes (*Vitis vinifera* L.). As reference measurements, the flavanol content was estimated using the *p*-dimethylaminocinnamaldehyde (DMACA) method. Not only total flavanol content was evaluated but also the quantity of flavanols that would be extracted into the wine during winemaking. A like-wine model solution was used for this purpose. Calibrations were performed by partial least squares regression and they provide coefficients of determination $R^2=0.73$ for total flavanol content and $R^2=0.85$ for predicting flavanols extracted with model solution. Values up to $R^2=0.88$ were reached when cultivars were considered individually.

1. Introduction

Grape seeds constitute a small part of the berry, but they affect extensively the sensory properties of wine. Their phenolic compounds are responsible of these properties and they change in a qualitative and quantitative manner during ripening [1,2]. The most representative of them in grape seeds, flavanols, include flavan-3-ol monomers (catechin, epicatechin and epicatechin gallate) and procyanidins, which are polymers comprised of flavan-3-ol terminal and extension subunits [3]. Phenolic composition of grapes depends on multiple factors, including climate, variety, soil, and degree of ripeness, being this phenolic maturity decisive for the production of quality red wines. Although seeds represent only 0–6% of berry weight, they are an important source of flavanols for wines. Another aspect that has raised interest is the extractability of these compounds. It has been reported that extractability depends on the ripeness of grape seeds. This phenomenon is due to changes in the interactions between tannins and cell wall material [4]. Insufficiently ripened grapes have higher tannin extractability [5].

The determination of flavanols might help on the decision of the harvest date. However, the 'optimal' harvest date should be defined based on several measurements. Since changes during ripening affect both gustatory and appearance properties, sensorial analysis is the most common approach to evaluate the condition of the seeds by vine growers, though it is difficult to be carried out in an accurate and objective manner [6]. Some studies have found clear evidences relating chemical composition and sensorial parameters in vine products. In particular, flavanols are responsible of these properties in grape seeds [7,8]. Nevertheless, these methods frequently are destructive, time-consuming, and entail the use of reagents [9–12]. Replacing conventional analyses, near infrared (NIR) spectroscopy provides fast, accurate and non-destructive way to obtain chemical composition [13,14]. These techniques have been successfully joined to computer vision systems [15,16]. NIR radiation has very little energy and penetrates a millimetre or so into the substance depending on the substance's surface composition and structure. Anyhow, phenolic compounds are mainly concentrated within the outer layer of grape seeds [17].

Near-infrared (NIR) hyperspectral imaging is a powerful technique which has been used in several applications in agricultural products [18–22]. In fact, it has been applied to grape seeds for establishing the methodology for acquiring images, discriminating varieties and estimating the date of sampling, but not yet for predicting chemical composition [23]. Hyperspectral imaging provides a digital image and the spectrum belonging to each pixel. Hyperspectral images (HSI), or hypercubes, are three-dimensional data matrix where the first two axes of the matrix represent the

* Corresponding author. Tel.: +34 954556495; fax: +34 954556110.
E-mail address: heredia@us.es (F.J. Heredia).

0039-9140/$ - see front matter © 2014 Elsevier B.V. All rights reserved.
http://dx.doi.org/10.1016/j.talanta.2014.01.044

spatial coordinates, while the third axis portrays the spectral dimension. They usually are represented as a battery of images where each layer shows the reflectance at a wavelength in grey scale [24]. Due to the great amount of information that they include, HSI require the application of multivariate data analysis for data exploration. As with NIR spectroscopy, chemometric techniques are applied to decompose the image dataset, process and perform regression or classification analyses. The possibilities of hyperspectral imaging based on the NIR range have been illustrated developing a model able to predict and classify barley kernels [25,26], predicting hardness in maize kernels [27], and studying enzymes activity and detecting sprout damage in wheat [28,29].

In order to minimise contributions from imaging instrument responses that are not related to variations in the composition of the imaged sample, preprocessing of spectral data is often of vital importance if reasonable results are to be obtained from the spectral analysis step. The most frequently used methods for spectral correction are multiplicative scatter correction (MSC), standard normal variate (SNV) and derivation [30–33]. However, there is still no standard procedure to decide which spectral processing produce best results. Partial least squares regression (PLSR) is a procedure used to relate a large number of independent variables (predictors) to one (PLSR1) or few (PLRS2) response variables (observations) when a reduced number of cases are available. Since it reduces a great number of redundant information, it is very effective in spectral analysis [34,35].

The aim of this work was to evaluate the potential of NIR hyperspectral imaging for the evaluation of flavanols in seeds from red and white grapes during ripening. Hyperspectral imaging was chosen as the best option for evaluating reflectance spectrum in grape seeds because of their heterogeneity and reduced size. Measurements by bulk NIR spectroradiometry need an amount of sample that covers the whole spot of measurement. In this case, the seeds contain interstitial spaces that produce shadows affecting the spectrum intensity. Imaging techniques allow measuring a maximum area of sample without the influence of shadows.

2. Material and methods

2.1. Sampling

The grapes (*Vitis vinifera* L.) sampled are included under the "Condado de Huelva" Designation of Origin, in Southwestern Spain, harvested in 2012. One red variety (cv. Tempranillo) and one autochthonous white variety (cv. Zalema) were used. The number of samples was 18 for Zalema and 15 for Tempranillo, depending on the availability and harvesting times of each variety. They were taken twice a week from early July until postharvest mid-September. Sampling process was carried out at daybreak by taking a pair of berries from alternate grapevines, from four rows of vines, and from both sides of each row up to reach 2 kg of berries. In this process, the berries were taken with pedicel intact to slow down the berry oxidation as long as possible. Once in laboratory, one hundred berries were randomly taken and seeds removed, left to dry at room temperature for 2 h, and frozen at −20 °C until acquisition of hyperspectral images and chemical analysis. Each sample was divided into three parts used as replicates ((18+15)×3=99 samples). Two of these replicates were allocated to the calibration set and the other sample to the prediction set.

2.2. Hyperspectral image analysis

The system comprised a Xenics® XEVA-USB InGaAs camera (320×256 pixels; Xenics Infrared Solutions, Inc., Leuven, Belgium), a spectrograph (Specim ImSpector N17E Enhanced; Spectral Imaging Ltd., Oulu, Finland) covering the spectral range between 884 and 1717 nm (spectral resolution of 3.25 nm), two 70 W tungsten iodine halogen lamps (Prilux®, Barcelona, Spain) used as light source, a mirror scanner (Spectral Imaging Ltd., Oulu, Finland), and a computer system. HSI were recorded using a 50 Hz frame rate and an exposure time of 9 ms using the instrument acquisition software SpectralDAQ 3.62 (Spectral Imaging Ltd., Oulu, Finland). From the acquired HSI, it was observed that the first and the last twenty bands of the image had a high level of noise, thus not being useful for spectral data extraction. Therefore, images were cropped to the spectral range of 950–1650 nm with a total of 215 bands.

A 'white reference' image (W, 100% reflectance) was acquired from a white Spectralon® ceramic tile (Labsphere Inc., North Sutton, USA), and a 'dark reference' image (B, 0% reflectance) was obtained with the light source off and the mirror scanner completely covered with its opaque cap. The white and dark 'reference' HSI were used to correct the raw images (R_0) in order to obtain a relative reflectance image (R) according to the following equation:

$$R = \frac{R_0 - B}{W - B} \quad (1)$$

For segmentation of HSI, a method based on forward stepwise discriminant analysis was applied with the software Statistica 8.0 [36]. Image processing, spectral processing and statistical treatment were carried out using MATLAB R2012b [37]. A flowchart of the image processing and spectral treatment used in this study is schematized in Fig. 1.

2.3. Chemical analysis

Each sample was split into two fractions subjected to different extractions. For the exhaustive extraction, grape seeds were freeze-dried and ground to obtain a homogeneous powder for extraction. One gram of seed powder was extracted with 10 mL of methanol:water (75:25), sonicated (15 min) and centrifuged (15 min), repeating the extraction process twice more. The methanolic extracts were combined and finally made up to 50 mL with methanol. For the extraction in wine-like medium, two grams of intact grape seeds were macerated in 50 mL of model wine solution (4 g L^{-1} tartaric acid, 12.5% ethanol, adjusted at pH 3.6 with NaOH 0.5 M) during 72 h [38].

Flavanols spectrophotometric analysis of both extractions was carried out following a modification of Vivas et al. [39]. Ten or twenty microlitres of total extraction or wine like medium extracts were mixed with 190 or 180 μL of methanol respetively and 1 mL of DMACA reagent. The DMACA reagent was prepared immediately before use, containing 0.1% (w/v) DMACA (4-dimethylaminocinnamaldehyde) in a mixture of HCl:methanol (1:10, v/v). The analyses were performed in triplicate on an Agilent 8453 UV–visible spectrophotometer (Palo Alto, USA), equipped with diode array detection (DAD), measuring absorbance at 640 nm and using a calibration curve of (+)-catechin (Sigma-Aldrich, St. Louis, USA) for quantification. The aforesaid extract volumes were appropriately modified when the concentration was outside the linear range of the calibration curve. All results were expressed as mg of catechin equivalents per gram of grape seed.

3. Results and discussion

3.1. Segmentation by discriminant analysis

A set of reflectance spectra belonging to seeds and background was collected as input data set. The forward stepwise discriminant analysis included sequentially three wavelengths, 1216, 1392, and

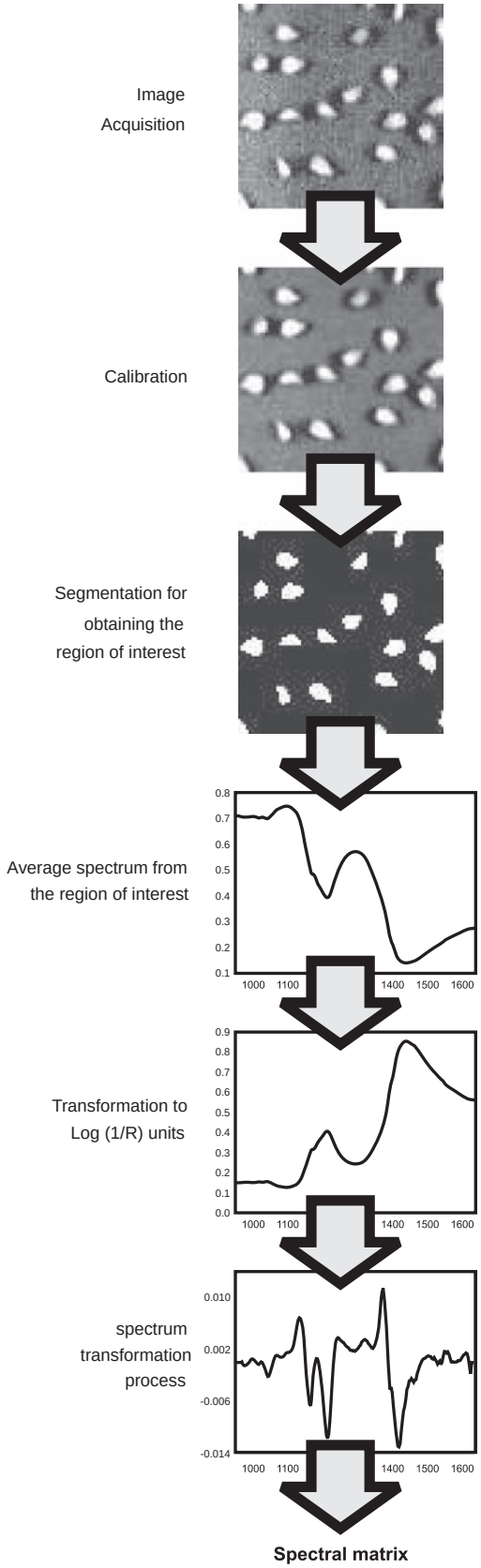

Fig. 1. Flow chart of the image processing and spectral treatment used in this study.

1147 nm for discriminating the region of interest from the background. Fig. 2 shows the average spectra belonging to seeds and background (a homogeneous surface composed of polyethylene)

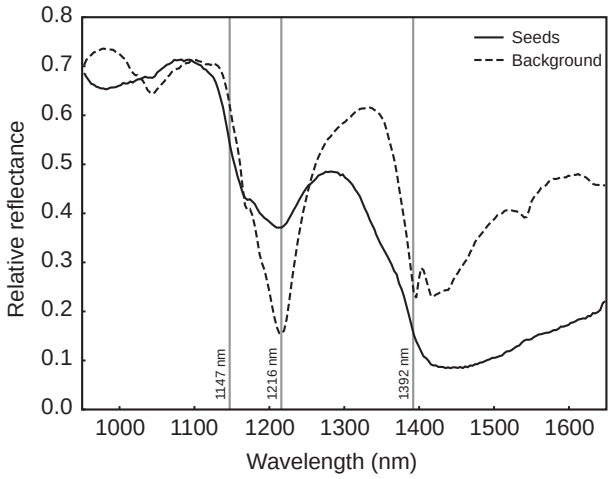

Fig. 2. Spectra of seeds and background highlighting the bands included by the forward stepwise discriminant analysis.

and highlights the selected bands. The algorithm of segmentation saved all the masks of segmentation and they were visually supervised for ensuring the suitability of the proposed method.

3.2. Exploratory analysis of spectra

Fig. 3 shows the mean and standard deviation spectra regarding the variety of grape seeds. It also shows the spectra after applying the transformations Log(1/*R*), SNV treatment, and second derivative, treatments that yielded the best results in prediction analyses. It can be seen that seeds from white and red grapes have different reflectance intensities along some wavelength regions, although with the same pattern.

Before the quantitative analysis, principal component analysis (PCA) was used as unsupervised pattern recognition technique in order to get information about the latent structure of the spectral matrix. This method provided not only information related to spectral outliers and the distribution of samples in the newly-created space but also was an important source of knowledge with which to evaluate the suitability of prediction set used in PLSR. For detecting possible outliers, Hotelling's T^2 statistic was used as a measure of the multivariate distance of each sample from the centre of the data set [40]. Regarding the spectral features of each sample, this test rejected 4 of the 99 samples considering a confidence level of 95%. Using the spectral data of the remaining samples (without outliers), PCA was applied again in order to ensure the representativeness of the prediction set in the generated multivariate space.

PC1, PC2, and PC3 explained 98.61%, 1.18%, and 0.10% of the total variance respectively. PC1 was influenced by the time in an extensively manner. Fig. 4a shows PC1 and its evolution over time. At every date, spectra from Tempranillo seeds had higher scores than Zalema ones. Moreover, this dependency seemed stronger for Tempranillo, being its slope higher. Fig. 4b shows the scatterplot of scores for PC2 and PC3. Generally, Tempranillo seeds presented positive scores for PC2 while Zalema seeds presented negative ones. Furthermore, it can be observed that samples belonging to prediction set were uniformly distributed among calibration set samples. These results are in agreement with results previously reported [23].

3.3. Quantitative analysis

Flavanols content decreased during the grape ripening regardless the variety and type of extraction. The methanol extract

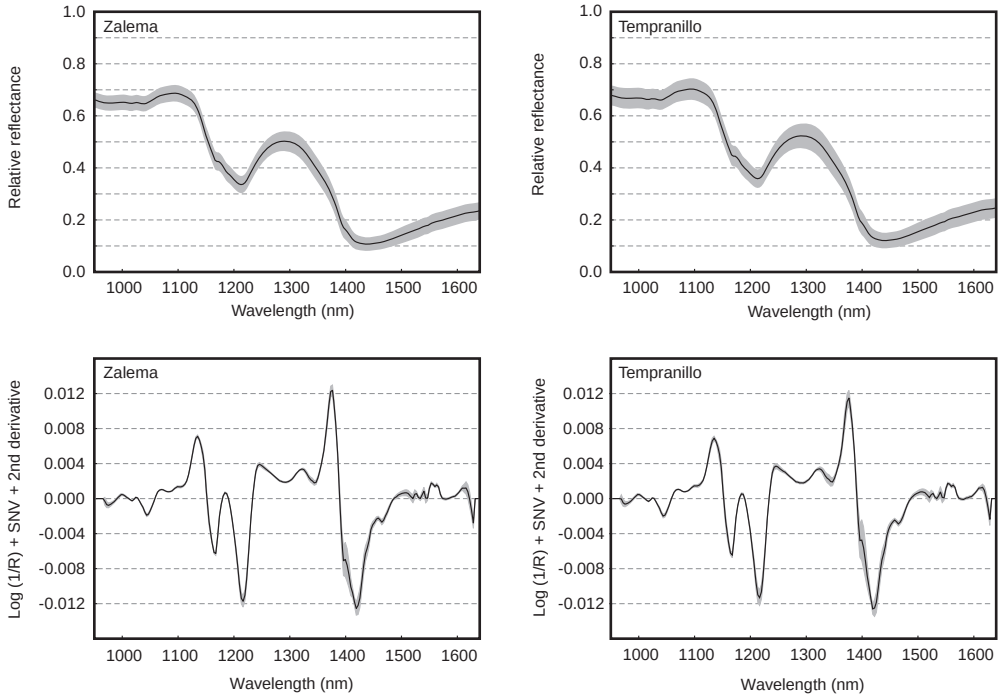

Fig. 3. Average reflectance spectra and average processed spectra of each variety. Shaded areas represent the standard deviation at each wavelength.

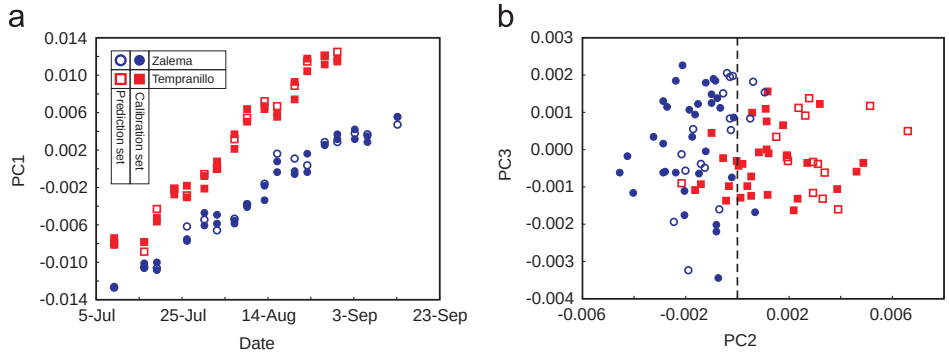

Fig. 4. (a) Dependency of PC1 with date. (b) Scatterplot of scores for PC2 and PC3. Circles represent Zalema and squares represent Tempranillo, in turn, filled and unfilled marks belong to calibration and prediction sets respectively.

flavanols ranged from 4.28 to 34.26 mg g^{-1} of grape seed. The flavanols from the extracts obtained using like-wine solution ranged from 0.12 to 7.21 mg g^{-1} of grape seed. Table 1 shows a brief resume of the aforementioned results. It must be highlighted that high standard deviations were due to the evolution during ripeness instead of errors of measurements. Although it was not the goal of this work, extractability of each sample was evaluated as the fraction of flavanols extracted by the model solution with respect to the exhaustive extraction. The extractability also decreased during ripening, being about 25% at the first stages and about 5% in the last ones.

Results of chemical analyses were used as dependent (Y) variables and the matrix of processed spectra was used as the independent (X) variables in the PLSR. The statistical parameters of the final calibration equations are shown in Table 2. For extractions with methanol and considering all samples as a unique data set, R^2 was 0.73 for calibration and 0.75 for prediction. The RMSEC and RMSEP were 4.01 and 3.86 mg g^{-1} of grape seed respectively. Results for predicting flavanols extracted by like-wine solution had R^2=0.82 for calibration and R^2=0.85 for prediction. In this case, RMSEC and RMSEP were 0.92 and 0.88 mg g^{-1} of grape seed respectively. Since cultivar was a determining factor in the preliminary exploratory analysis, the PLSR were repeated for each variety individually. Because of this, results in Tables 1 and 2 are also broken down into varieties. As it was expected, coefficients of determination increased while RMSEC and RMSEP decreased.

Table 1
Summary of chemical analyses for all samples and regarding the variety (all results were expressed as mg of catechin equivalents per gram of grape seed).

	N	Extraction	Mean	Minimum	Maximum	Std. dev.
All samples	95	Model wine	2.26	0.12	7.21	2.22
		Total	15.82	4.28	34.26	7.74
Zalema	50	Model wine	2.54	0.38	6.48	2.40
		Total	15.85	5.63	28.05	6.93
Tempranillo	45	Model wine	1.95	0.12	7.21	1.98
		Total	15.78	4.28	34.26	8.63

Fig. 5 shows the loadings resulting of the PLSR model for total flavanols and it indicates the most dominant wavelengths. The spectral region between 1100 and 1300 nm showed important contribution to the model loadings and is mainly related to the combination band of O–H symmetric and anti-symmetric stretching vibration, the combination band of C–H aromatic second

Table 2
Calibration and prediction results for the PLS models obtained from processed spectra (all results were expressed as mg of catechin equivalents per gram of grape seed).

	N	Extraction	PLS factors	R_C^2	RMSEC	R_P^2	RMSEP
All samples	95	Model wine	3	0.82	0.92	0.85	0.88
		Total	3	0.73	4.01	0.75	3.86
Zalema	50	Model wine	2	0.83	0.98	0.85	0.92
		Total	1	0.82	2.90	0.82	2.93
Tempranillo	45	Model wine	2	0.88	0.67	0.88	0.69
		Total	6	0.94	2.09	0.88	2.89

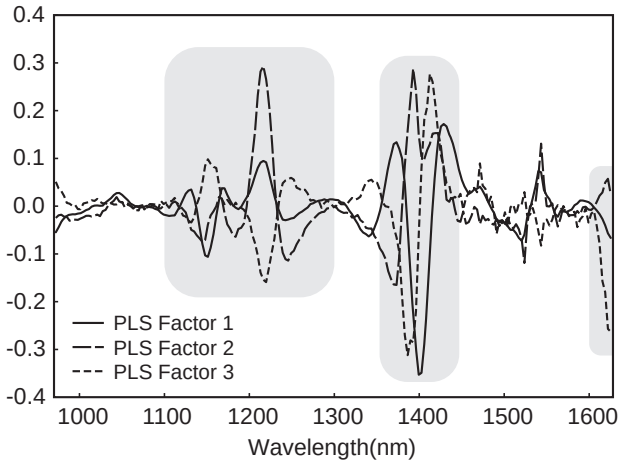

Fig. 5. Loadings plot for the first three PLS factors of the regression model for total flavanols prediction.

overtone, and C–H third overtone vibration. These can be attributed to the chemical structure of phenolic compounds [41,42]. The first O–H stretching overtone contributes to spectrum at 1400 nm, hence the moisture affects expansively to this band. In this case, the influence can be attributed to the loss of water that grape seeds suffer at the same time that flavanols develop [43]. According to Goodchild et al. [44], bands close to 1600 nm are attributed to condensed tannins.

4. Conclusions

The PLSR models were successfully performed to evaluate flavanols in grape seeds. These were able to predict the concentration of flavanols of a sample based on spectral features as the predictor variables with a coefficient of determination of R^2 of 0.75 for total extractions and 0.85 for extractions with model wine solution. Furthermore, this coefficient reached up to 0.88 when varieties were considered individually. On the other hand, PCA was suitable for grape seeds characterization regarding the variety, proving the suitability of the methodology previously established.

It is well known that in the case of agricultural products the range of the variability should be as large as that expected in any future samples. In this work, seeds from different cultivars have been collected during ripening; therefore this variability should be enough to develop models in a feasibility study. Nonetheless, a comprehensive study must be made in order to evaluate other factors such as different production areas, vintages and varieties, for the complete development of these models. Though it is not yet a substitute for conventional chemical analysis, it arises as an attractive alternative due to its simplicity and quickness. By establishing the variables that affects each cultivar, this could become a reference method to assess the chemical characteristics of grape seeds during maturation, being very useful for vine growers and wineries.

Acknowledgements

This work was supported by the projects P10-AGR6331 (Consejería de Economía, Innovación, Ciencia y Empresa, Junta de Andalucía), AGL2011-30254-C02 (Ministerio de Economía y Competitividad, Gobierno de España). The Spanish MICINN is also thanked for F.J. Rodríguez-Pulido, J. Nogales-Bueno FPI grants (BES-2009-025429 and BES-2012-060192 respectively) and J.M. Hernández-Hierro 'Juan de la Cierva' contract (JCI-2011-09201).

References

[1] Y. Cadot, M.T. Miñana-Castelló, M. Chevalier, J. Agric. Food Chem. 54 (2006) 9206–9215.
[2] B.S. Sun, T. Pinto, M.C. Leandro, J.M. Ricardo-Da-Silva, M.I. Spranger, Am. J. Enol. Vitic 50 (1999) 179–184.
[3] R. Ristic, P.G. Iland, Aust. J. Grape Wine Res. 11 (2005) 43–58.
[4] R.L. Hanlin, M. Hrmova, J.F. Harbertson, M.O. Downey, Aust. J. Grape Wine Res. 16 (2010) 173–188.
[5] C. Peyrot des Gachons, J.A. Kennedy, J. Agric. Food Chem. 51 (2003) 5877–5881.
[6] J. Rousseau, D. Delteil, Revue française d'oenologie 183 (2000) 10–13.
[7] R. Gawel, Aust. J. Grape Wine Res. 4 (1998) 74–95.
[8] R. Ferrer-Gallego, M. García-Marino, J.M. Hernández-Hierro, J.C. Rivas-Gonzalo, M.T. Escribano-Bailón, Anal. Chim. Acta 660 (2010) 22–28.
[9] A.K. Sandhu, L. Gu, J. Agric. Food Chem. 58 (2010) 4681–4692.
[10] T. Fuleki, J.M. Ricardo da Silva, J. Agric. Food Chem. 45 (1997) 1156–1160.
[11] J.A. Kennedy, M.A. Matthews, A.L. Waterhouse, Phytochemistry 55 (2000) 77–85.
[12] E. Obreque-Slier, A. Peña-Neira, R. López-Solís, F. Zamora-Marín, J.M. Ricardo-da Silva, O. Laureano, J. Agric. Food Chem. 58 (2010) 3591–3599.
[13] B.M. Nicolaï, K. Beullens, E. Bobelyn, A. Peirs, W. Saeys, K.I. Theron, J. Lammertyn, Postharvest Biol. Technol. 46 (2007) 99–118.
[14] J.M. Hernández-Hierro, J. Valverde, S. Villacreces, K. Reilly, M. Gaffney, M.L. González-Miret, F.J. Heredia, G. Downey, J. Agric. Food Chem. 60 (2012) 7352–7358.
[15] D.F. Barbin, G. ElMasry, D.W. Sun, P. Allen, Food Chem. 138 (2013) 1162–1171.
[16] D.W. Sun, J. Food Eng. 61 (2004) 1–2.
[17] J.H. Thorngate, V.L. Singleton, Am. J. Enol. Vitic. 45 (1994) 259–262.
[18] T.M. Baye, T.C. Pearson, A.M. Settles, J. Cereal Sci. 43 (2006) 236–243.
[19] M.A. Shahin, S.J. Symons, Comput. Electron. Agric. 75 (2011) 107–112.
[20] S. Cubero, N. Aleixos, E. Moltó, J. Gómez-Sanchis, J. Blasco, Food Bioprocess Technol. 4 (2011) 487–504.
[21] D. Lorente, N. Aleixos, J. Gómez-Sanchis, S. Cubero, O.L. García-Navarrete, J. Blasco, Food Bioprocess Technol. 5 (2012) 1121–1142.
[22] A. Baiano, C. Terracone, G. Peri, R. Romaniello, Comput. Electron. Agric. 87 (2012) 142–151.
[23] F.J. Rodríguez-Pulido, D.F. Barbin, D.W. Sun, B. Gordillo, M.L. González-Miret, F.J. Heredia, Postharvest Biol. Technol. 76 (2013) 74–82.
[24] J. Burger, P. Geladi, Analyst 131 (2006) 1152–1160.
[25] L. Munck, B. Møller, J. Inst. Brew. 110 (2004) 3–17.
[26] P. Engelbrecht, M. Manley, P.J. Williams, G.D. Toit, P. Geladi, Pre-germination detected in whole cereal grains using near infrared hyperspectral imaging, in: Proceedings of the CST SA—ICC International Grains Symposium, Quality and Safety of Grain Crops and Foods, 2010, 123-127.
[27] P. Williams, P. Geladi, G. Fox, M. Manley, Anal. Chim. Acta 653 (2009) 121–130.
[28] J. Xing, S. Symons, M. Shahin, D. Hatcher, Biosystems Eng. 106 (2010) 188–194.
[29] J. Xing, P. Van Hung, S. Symons, M. Shahin, D. Hatcher, Sens. Instrum. Food Qual. Saf. 3 (2009) 211–218.
[30] P. Geladi, D. MacDougall, H. Martens, Appl. Spectrosc. 39 (1985) 491–500.
[31] T. Isaksson, T. Næs, Appl. Spectrosc. 42 (1988) 1273–1284.
[32] M. Kaihara, T. Takahashi, T. Akazawa, T. Sato, S. Takahashi, Spectrosc. Lett. 35 (2002) 369–376.
[33] C. Pizarro, I. Esteban-Díez, A.J. Nistal, J.-M. González-Sáiz, Anal. Chim. Acta 509 (2004) 217–227.
[34] P. Lin, Y. Chen, Y. He, Food Bioprocess Technol. 5 (2012) 235–242.
[35] M.M. Pojic, J.S. Mastilovic, Food Bioprocess Technol. 6 (2013) 330–352.
[36] StatSoft Inc. Statistica 8.0. 2007. Tulsa, USA, StatSoft Inc.
[37] The Mathworks. MATLAB R2012b. 2012. Natik, USA, The MathWorks Inc.
[38] A.B. Bautista-Ortín, P. Rodríguez-Rodríguez, R. Gil-Muñoz, E. Jumínez-Pascual, N. Busse-Valverde, A. Martínez-Cutillas, J.M. López-Roca, E. Gómez-Plaza, Aust. J. Grape Wine Res. 18 (2012) 123–130.
[39] N. Vivas, Y. Glories, L. Lagune, C. Saucier, M. Augustin, Journal International des Sciences de la Vigne et du Vin 28 (1994) 319–336.
[40 J.E. Jackson, A User's, Guide to Principal Components, Wiley, 2005.

[41] L. Bokobza, Near-Infrared Spectroscopy: Principles, Instruments, in: H.W. Siesler, Y. Ozaki, S. Kawata, H.M. Heise (Eds.), Applications, Wiley-VCH Verlag GmbH, Weinheim, Germany, 2007, pp. 11–41.
[42] R. Ferrer-Gallego, J.M. Hernández-Hierro, J.C. Rivas-Gonzalo, M.T. Escribano-Bailón, LWT Food Sci. Technol. 44 (2011) 847–853.
[43] B.G. Osborne, T. Fearn, P.T. Hindle, Practical NIR Spectroscopy With Applications in Food and Beverage Analysis, Longman Group, United Kingdom, 1993.
[44] A.V. Goodchild, F.J. El Haramein, A. Abd El Moneim, H.P.S. Makkar, P.C. Williams, J. Near Infrared Spectrosc. 6 (1998) 175–181.